

# Enhanced Fuzzy Sliding Mode Control to Motion Controller of Linear Induction Motor Drives

Kou-Cheng Hsu\*, Hsin-Han Chiang\*, Guan-Hua Huang\*, Tsu-Tian Lee\*\*

\* Dept. Electrical Engineering, Fu Jen Catholic University, New Taipei City, Taiwan

\*\* Dept. Electrical Engineering, Chung Yung Christian University, Chung Li, Taiwan  
 035013@mail.fju.edu.tw, hsinhan@ee.fju.edu.tw, tlee@cycu.edu.tw

**Abstract**—In this paper, an enhanced fuzzy sliding mode control system (EFSMC) is proposed for a linear induction motor (LIM) to achieve the position tracking. First, the dynamic model of LIM is investigated for considering the end effect and the friction force into the observer-based compensation design to cope with the time-varying uncertainties. Then, a sliding mode control (SMC) based on the backstepping control technique is presented with the combination of two fuzzy logic controllers. The first fuzzy logic controller is proposed, through a dynamic tune of the sliding surface slope constant of the SMC according to the controlled system states by a fuzzy logic unit. To relax the need of the upper bound of the lumped uncertainties in the SMC, the second fuzzy logic controller is presented, in which the upper bound of the lumped uncertainties can be estimated by a fuzzy inference mechanism. Finally, the experiments for several scenarios are conducted to demonstrate the effectiveness and robustness of the designed controller.

**Keywords**—Sliding mode control, fuzzy control, observer, end effect, induction motor drives.

## I. INTRODUCTION

Linear induction motors (LIMs) have been widely used in many industrial applications. This is attributed to the various advantages of the LIM, including high starting thrust force, high precision, silence, no need for gear between motor and the motion devices, direct drive, simple mechanical construction, lower costs, high-speed operation, easy maintenance and high speed applications [1]. The driving principles of the LIM are similar to the traditional rotary induction motors (RIMs), but the motor parameters of LIMs are time-varying due to changes in operating conditions, such as the speed of mover, temperature, end effect, external disturbances and rail configuration [2]. Moreover, the operation of LIMs will inevitably produce a friction force between the two contacting bodies, and it is easily varied due to the temperature and humidity [3]. The above mentioned disadvantages raise the challenge to design a high grade controller for LIMs.

The end effect phenomenon, in a LIM system, inevitably degrades the performance of a LIM in tracking the reference trajectories. The end effect will also decrease efficiency, output force, power factor and unbalances the phase current [4]. Therefore, it should be reduced in the motion step to improve the tracking performance. To deal with the uncertainties, many researchers have proposed various approaches in the control field. Among them, sliding mode control (SMC) is one of the powerful methods to control nonlinear and uncertain systems [5]. However, the sliding surface slope and the uncertainty

boundary are difficult to obtain in the controller design of SMC in advance for practical applications. Moreover, the chattering phenomenon exists in the application of SMC systems. For practical application, SMC cannot be practically implemented due to this phenomenon which may lead to high frequency disturbance and cause unpredictable instabilities [6]. To this end, many studies have employed the controlled system states by a fuzzy logic unit to dynamically tune the sliding surface slope of the SMC (e.g., [7]). In [8], fuzzy inference mechanism is applied to estimate the upper bound of the uncertainties for SMC scheme. Besides, a fuzzy sliding mode system is proposed to construct a robust control law for a LIM drive [9]. However, the large amount of fuzzy sets raises the system operation complexity for a high-order system. Besides, the suitable membership function and the fuzzy control rules are usually selected by the trial error and experience, respectively. To overcome these problems, many research combining the fuzzy control with the SMC are still evolving toward the improved control scheme to confront the uncertainties that exists in a LIM drive while allowing possible reduced controller complexity and high performance applications.

The motivation of this paper is to design an enhanced fuzzy sliding mode controller (EFSMC) for LIM drives based on the sense of Lyapunov theorem and fuzzy logic control. Additionally, a flux observer is developed to estimate the secondary flux for the LIM and further to use the estimated flux to compensate the end effect phenomenon in the control law. Without need for high control gains in the conventional control approaches, our system can achieve the high precision motion performance.

## II. LIM DRIVE MODEL

In the control of a LIM, the indirect field-oriented control technique is one of the popular control schemes widely used in LIM drive control. The main idea of the indirect field-oriented control for LIM is the decoupling feature of the flux amplitude and the thrust force. The flux orientation can be obtained by forcing the secondary flux vector aligning with the d-axis, and it can be realized by setting the secondary flux of d-axis and of q-axis to a constant value and zero, respectively. Accordingly, based on the d-axis and q-axis theory, the dynamic model of the LIM drive can be expressed as follows [10]:

$$i_{qs} = -\left(\frac{R_s}{L_\sigma L_s} + \frac{1-L_\sigma}{L_\sigma T_r}\right) i_{qs} - \frac{n_p L_m \pi}{L_\sigma L_s L_r h} v \lambda_{dr} + \frac{L_m}{L_\sigma L_s L_r T_r} \lambda_{qr} + \frac{1}{L_\sigma L_s} V_{qs} \quad (1)$$

$$i_{ds} = -\left(\frac{R_s}{L_\sigma L_s} + \frac{1-L_\sigma}{L_\sigma T_r}\right) i_{ds} + \frac{L_m}{L_\sigma L_s L_r T_r} \lambda_{dr} + \frac{n_p L_m \pi}{L_\sigma L_s L_r h} v \lambda_{qr} + \frac{1}{L_\sigma L_s} V_{ds} \quad (2)$$

$$\dot{\lambda}_{qr} = \frac{L_m}{T_r} i_{qs} - \frac{1}{T_r} \lambda_{qr} + n_p \frac{\pi}{h} v \lambda_{dr} \quad (3)$$

$$\dot{\lambda}_{dr} = \frac{L_m}{T_r} i_{ds} - \frac{1}{T_r} \lambda_{dr} - n_p \frac{\pi}{h} v \lambda_{qr} \quad (4)$$

$$M\dot{v} = K_f (\lambda_{dr} i_{qs} - \lambda_{qr} i_{ds}) - F_L - F_r = F_e - F_L - F_r \quad (5)$$

where  $T_r = L_r / R_r$ ,  $L_\sigma = 1 - (L_m^2 / L_s L_m)$ ,  $K_f = 3n_p \pi L_m / (2hL_r)$ ,  $R_s$  is the primary resistance per phase,  $R_r$  is the secondary resistance per phase,  $L_m$  is the magnetizing inductance per phase,  $L_s$  is the primary inductance per phase,  $L_r$  is the secondary inductance per phase,  $v$  is the mover velocity,  $v_e$  is the synchronous linear velocity,  $h$  is the pole pitch,  $n_p$  is the number of pole pairs,  $\lambda_{dr}$  and  $\lambda_{qr}$  are d-axis and q-axis secondary flux, respectively;  $i_{ds}$  and  $i_{qs}$  are d-axis and q-axis primary current, respectively;  $V_{ds}$  and  $V_{qs}$  are d-axis and q-axis primary voltage, respectively;  $T_r$  is the secondary time constant,  $L_\sigma$  is the leakage coefficient,  $K_f$  is the force constant,  $F_e$  is the electromagnetic force,  $F_L$  is the external force disturbance, and  $M$  is the total mass of the moving element. The frictional force  $F_r$  can be formulated by using the Lu Gre friction model [11], and then the dynamics of friction force model can be obtained as:

$$\frac{df_s}{dt} = v - \frac{|v|}{n(v)} f_s \quad (6)$$

$$F_r = \zeta_0 f_s + \zeta_1 \frac{df_s}{dt} + \zeta_2 v \quad (7)$$

where  $f_s$  is the friction state, in terms of the average deflection of the bristles among the two contact surfaces;  $\zeta_0$  is the stiffness of bristles,  $\zeta_1$  is the damping coefficient, and  $\zeta_2$  is the viscous coefficient. These three parameters are defined as unknown positive constants. In addition,  $n(v)$  is assumed to be known to describe the Stribeck effect [11]:

$$n(v) = F_c + (F_s - F_c) e^{-(v/v_s)^2} \quad (8)$$

where  $F_c$  is the Coulomb friction value,  $F_s$  is the static friction force value, and  $v_s$  is the Stribeck velocity.

Due to the end effects, the time constant becomes larger for the currents decaying more slowly in the linear motor at the entry end than that at the exit end. We use the parameter  $Q$  to simulate the end effect phenomenon expressed as [12]:

$$Q = lR_r / (L_r v) \quad (9)$$

where  $l$  is the primary length. Thus, we can define the magnetizing inductance as below:

$$L'_m = L_m(Q) = L_m(1 - f(Q)) \quad (10)$$

where  $f(Q) = (1 - e^{-Q})/Q$ . The primary and secondary inductances are expressed as [12]:

$$L'_s = L_s(Q) = L_s - L_m f(Q) \quad (11)$$

$$L'_r = L_r(Q) = L_r - L_m f(Q) \quad (12)$$

Moreover, the secondary time constant is given by

$$T'_r = \frac{L'_r}{R_r} = \frac{L_r}{R_r} - \frac{L_m \cdot f(Q)}{R_r} \quad (13)$$

Then, by the assumption that the reference frame is aligned with the secondary flux, it follows that  $\lambda_{qr} = 0$

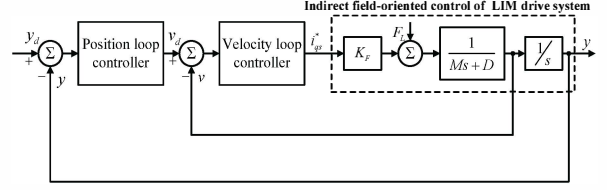


Fig. 1. Block diagram of the LIM drive system.

and  $\dot{\lambda}_{qr} = 0$ ; the desired secondary flux linkage in terms of  $i_{ds}$  can be resulted as follows:

$$\lambda_{dr} = \frac{L_m / T_r}{s + 1 / T_r} i_{ds} \quad (14)$$

where  $s$  is the Laplace operator. Furthermore, the feedforward slip velocity signal can be estimated as follows:

$$v_{sl} = \frac{hL'_m}{\pi T'_r} \cdot \frac{i_{qs}}{\lambda_{dr}} = \frac{hL_m(1 - f(Q))}{\pi(L_r / R_r - L_m f(Q) / R_r)} \cdot \frac{i_{qs}}{\lambda_{dr}} \quad (15)$$

Then, by using the indirect field-oriented control scheme, the electromagnetic force shown in (5) can be represented by the following equations:

$$F_e = K_F i_{qs} \quad (16)$$

$$K_F = \frac{3}{2} n_p \frac{\pi [L_m(1 - f(Q))]^2}{h(L_r - L_m f(Q))} i_{ds} \quad (17)$$

In addition, the simplified indirect field-oriented control of a LIM drive system can be depicted in Fig. 1, in which  $y$  is the mover position,  $y_d$  is the reference trajectory and  $v_d$  is the reference velocity.

### III. OBSERVER DESIGN FOR END EFFECT COMPENSATION

In this section, in order to obtain the accurate value of fluxes, a flux observer is proposed to estimate the secondary flux for the LIM. Moreover, the estimated secondary flux will be a part of the compensator for end effect phenomenon to further improve the tracking performance of the LIM.

Before designing the observer, we have to consider the following assumptions:

- A. 1: three phases are balanced.
- A. 2: the magnetic circuit is unsaturated.
- A. 3: there is no end effect.
- A. 4:  $\lambda_{qr}^2 + \lambda_{dr}^2 > 0$ .

Then further simplify the LIM dynamics in (1)-(4) by using a nonlinear coordinate transformation given as follows:

$$a_1 = i_{qs}^2 + i_{ds}^2 \quad (18)$$

$$a_2 = \lambda_{qr}^2 + \lambda_{dr}^2 \quad (19)$$

$$a_3 = i_{qs} \lambda_{qr} + i_{ds} \lambda_{dr} \quad (20)$$

$$a_4 = i_{qs} \lambda_{dr} - i_{ds} \lambda_{qr} \quad (21)$$

$$a_5 = v \quad (22)$$

Under the given assumptions above, all the states are measurable except the secondary flux. Thus, we have to design a flux observer to estimate the secondary flux. The following observers are designed as:

$$\dot{\hat{\lambda}}_{qr} = \frac{L_m R_r}{L_r} i_{qs} - \frac{R_r}{L_r} \hat{\lambda}_{qr} + \left( n_p \frac{\pi}{h} \right) v \hat{\lambda}_{dr} \quad (23)$$

$$\dot{\hat{\lambda}}_{dr} = \frac{L_m R_r}{L_r} i_{ds} - \frac{R_r}{L_r} \hat{\lambda}_{dr} - \left( n_p \frac{\pi}{h} \right) v \hat{\lambda}_{qr} \quad (24)$$

According to the contention of [13], if all the states are measurable except the secondary flux, and moreover, all the parameters are assumed to be known already. Then, the designed flux observer can guarantee that  $\hat{\lambda}_{ci} - \lambda_{ci} \rightarrow 0$  and  $\hat{\lambda}_q - \lambda_q \rightarrow 0$  as  $t \rightarrow \infty$ .

The object of the estimator is to provide the compensation amount in the LIM control law and then improve the tracking performance of the LIM. The proposed method makes use of the inverse secondary time constant to calculate the variation caused by the end effect especially at high speed. There are two design objects of the estimator for inverse secondary time constant, that is, one is to get a correct initial estimation and the other is to track the changes of the secondary time constant on the motor side. From (13), (23), and (24), we can rewrite the flux observer with the end effect phenomenon as:

$$\dot{\hat{\lambda}}_{qr} = L'_m \bar{T}'_r i_{qs} - \bar{T}'_r \hat{\lambda}_{qr} - v_{sl} \frac{\pi}{h} \hat{\lambda}_{dr} \quad (25)$$

$$\dot{\hat{\lambda}}_{dr} = L'_m \bar{T}'_r i_{ds} - \bar{T}'_r \hat{\lambda}_{dr} + v_{sl} \frac{\pi}{h} \hat{\lambda}_{qr} \quad (26)$$

where  $\bar{T}'_r = 1/T'_r$  denotes the inverse secondary time constant. The estimator uses the two estimated values of secondary flux from equations (25) and (26). The error of flux between reference and estimated secondary flux  $\Delta\lambda_r$  can be written as:

$$\Delta\lambda_r = |\lambda_r| - |\hat{\lambda}_r| \quad (27)$$

where  $|\lambda_r| = \sqrt{\lambda_{qr}^2 + \lambda_{dr}^2}$  and  $|\hat{\lambda}_r| = \sqrt{\hat{\lambda}_{qr}^2 + \hat{\lambda}_{dr}^2}$  denotes the reference and estimated secondary flux, respectively. Then the  $\Delta\lambda_r$  will be the input to a linear PI controller which produces the deviation in the inverse secondary time constant. The variation in the inverse secondary time constant related to  $\Delta\lambda_r$  is:

$$\Delta\bar{T}'_r = K_p \Delta\lambda_r + K_I \int \Delta\lambda_r dt \quad (28)$$

where  $K_p$  and  $K_I$  are the proportional and integral gains,  $\Delta\bar{T}'_r$  is the estimated change in the inverse secondary time constant. Furthermore,  $\bar{T}'_r$  is calculated by

$$\bar{T}'_r = \bar{T}'_r + \Delta\bar{T}'_r \quad (29)$$

Thus, we can use  $\bar{T}'_r$  to obtain the  $T'_r$  by the transformation of  $\bar{T}'_r = 1/T'_r$ . Moreover, in order to simplify the tuning algorithm, the variation of  $T'_r$  caused by the thermal drift of the secondary resistance  $R_r$  is neglected [12]. Figure 2 shows the update algorithm of the inverse secondary time constant. By (13), we can use the estimated value of secondary time constant  $T'_r$  to calculate the end effect variation as follow:

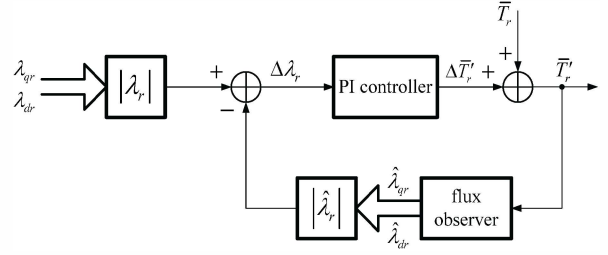


Fig. 2. The inverse secondary time constant estimator.

$$L_Q = L_m f(Q) = R_r (L_r / R_r - T'_r) \quad (30)$$

Subsequently, the value of end effect variation  $L_Q$  can be used to update the inductance values as follows:

$$L'_m = L_m - L_Q, \quad L'_r = L_r - L_Q, \quad L'_s = L_s - L_Q \quad (31)$$

These updated values of inductances and the estimated value of secondary time constant can be substituted into the slip velocity equation and the control law, as presented in the next section, to reduce the end effect phenomenon.

#### IV. ENHANCED FUZZY SLIDING MODE CONTROL DESIGN

Use either SI (MKS) or CGS as primary units. (SI units are encouraged.) English units may be used as secondary units (in parentheses). An exception would be the use of English units as identifiers in trade, such as "3.5-inch disk drive." Consider a LIM drive system with parameter variations, external disturbance and friction force, and the state variables defined as

$$x_1 = y, \quad x_2 = \dot{y} = v \quad (32)$$

then the associated state-space equations can be represented as

$$\begin{aligned} \dot{x}_1 &= \dot{y} \\ \dot{x}_2 &= (A + \Delta A)v + (B + \Delta B)u + C(F_L + F_r) \end{aligned} \quad (33)$$

where  $A = -\bar{D}/\bar{M}$ ,  $B = K_F/\bar{M}$ ,  $\Delta A$  and  $\Delta B$  are the uncertainties introduced by system parameters  $M$  and  $D$ ;  $u = i_{qs}$  is the control input to the motor drive system. Reformulating (33) yields:

$$\dot{x}_2 = Av + Bu + F \quad (34)$$

where  $F$  denotes the lumped uncertainty and is defined by

$$F \equiv \Delta Av + \Delta Bu + C(F_L + F_r) \quad (35)$$

Note that the lumped uncertainties can be reasonably assumed to be bounded, that is,  $|F(t)| \leq \eta$ .

Initially, the control objective is to design a SMC system for the output  $y$  to track the reference trajectory  $y_d$ . Note that  $y_d$  and its first two derivatives  $\dot{y}_d$ ,  $\ddot{y}_d$  are all bounded functions of time. The design step by using backstepping control method is presented as follows.

**Step 1:** For the position tracking objective, the tracking errors of the proposed sliding mode position controller are defined as follows:

$$e_y = y - y_d \quad (36)$$

and its derivative is

$$\dot{e}_y = \dot{y} - \dot{y}_d \quad (37)$$

The first Lyapunov function is chosen as

$$V_1 = e_y^2/2 \quad (38)$$

then the time derivative of  $V_1$  is

$$\dot{V}_1 = e_y \dot{e}_y = e_y (v - \dot{y}_d) \quad (39)$$

**Step 2:** Define the following Lyapunov function:

$$V_2 = V_1 + s^2/2 \quad (40)$$

with the sliding surface

$$s = ke_y + \dot{e}_y \quad (41)$$

where  $k$  is the slope constant of the sliding surface. Then the derivative of  $s$  is

$$\begin{aligned} \dot{s} &= k\dot{e}_y + \ddot{v} - \ddot{y}_d \\ &= k\dot{e}_y + Av + Bu + CF_L - \ddot{y}_d \end{aligned} \quad (42)$$

Differentiating (40) with respect to time and using (39) and (42), the derivative of  $V_2$  can be derived as

$$\begin{aligned} \dot{V}_2 &= \dot{V}_1 + s\dot{s} \\ &= e_y s - ke_y^2 + s(k\dot{e}_y + Av + Bu + CF_L - \ddot{y}_d) \\ &= e_y s - ke_y^2 + s[k\dot{e}_y + A(s + \dot{y}_d - ke_y) \\ &\quad + Bu + CF_L - \ddot{y}_d] \end{aligned} \quad (43)$$

According to (43), a backstepping sliding mode control law  $u$  can be designed as

$$u = B^{-1}[-e_y - k\dot{e}_y - A(s + \dot{y}_d - ke_y) + \ddot{y}_d - \eta \text{sgn}(s) - \gamma s] \quad (44)$$

where  $\eta$  and  $\gamma$  are positive constants. Substituting (44) into (43), the following result can be obtained:

$$\begin{aligned} \dot{V}_2 &= -ke_y^2 - \gamma s^2 + sCF_L - \eta|s| \\ &\leq -ke_y^2 - \gamma s^2 + (|CF_L| - \eta)|s| \\ &\leq -ke_y^2 - \gamma s^2 = -W(t) \leq 0 \end{aligned} \quad (45)$$

Define the following term

$$W(t) = ke_y^2 + \gamma s^2 \leq -\dot{V}_2(t) \quad (46)$$

Then

$$\int_0^\tau W(t)dt \leq -\int_0^\tau \dot{V}_2(t)dt = V_2(0) - V_2(\tau) \quad (47)$$

Because  $V_2(0)$  and  $V_2(\tau)$  are bounded, so the following result can be obtained:

$$\lim_{\tau \rightarrow \infty} \int_0^\tau W(t)dt < \infty \quad (48)$$

In addition,  $\dot{W}(t)$  is bounded, and  $W(t)$  is uniformly continuous. Using Barbalat's lemma, the following result can be obtained:

$$\lim_{t \rightarrow \infty} W(t) = 0 \quad (49)$$

Since  $k$ ,  $\gamma$  and  $W(t) = ke_y^2 + \gamma s^2$  are positive, from (49), one can obtain that the  $s(t)$  and  $e_y(t)$  will converge to zero as  $t \rightarrow \infty$ ; that is,  $\lim_{t \rightarrow \infty} y(t) = y_d$  and  $\lim_{t \rightarrow \infty} v(t) = \dot{y}_d$ . In summary, the backstepping-based SMC control law is asymptotically stable when parametric uncertainty, external force disturbance and/or friction force exist.

The conventional SMC employs discontinuous control to let the system state trajectories to lie within the sliding

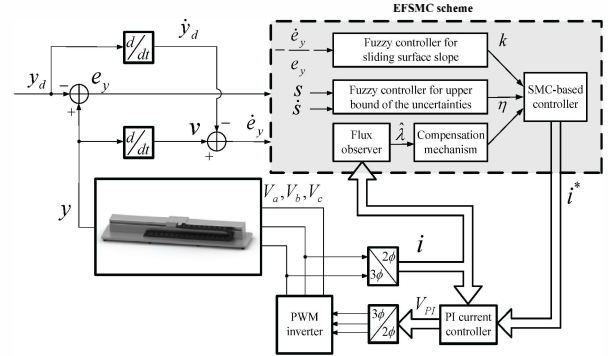


Fig. 3. Block diagram of the EFSMC control system.

surface, and this discontinuity control action will cause the chattering phenomenon which is undesirable in most applications. Besides, the state trajectory is sensitive to system uncertainty in the reaching phase. Thus, the convergence speed to the sliding surface will be asymptotic. These problems can be relaxed by using high-gain feedback to reduce the reaching time. The high-gain feedback, however, will cause some problems such as actuator saturation, extreme sensitivity to unmodeled dynamics. Finally, SMC requires the prior knowledge to the upper bound of the system uncertainties when it is used in the switching gain calculation. In order to overcome these drawbacks, EFSMC scheme is proposed which embeds two fuzzy logic units. One is to update the sliding surface slope  $k$  and the other is to dynamically adjust the switching control gain  $\eta$ .

The block diagram of the EFSMC system for a LIM drive is shown in Fig. 3. In this diagram, two fuzzy inference mechanisms are proposed to dynamically tune the control parameters. The scheme for tuning  $k$  can eliminate the problem of using high control gains in SMC so that the power consumptions of the motor drive are economically feasible. Besides, the fuzzy controller for tuning  $\eta$  can relax the requirement of determining the upper bound value of uncertainties in advance.

The main strategy of tuning the slope constant of the sliding mode controller is not to wait for the state errors to go to the sliding surface, but to drive the sliding surface to approach the state errors and make them zero as soon as possible. Because the sliding surface is near the axis of the state errors of the system, the control gains in the conventional SMC is no longer required with large values. the input fuzzy variable is the negative value of the ratio between the derivative of error and error of the controlled system state  $(-\dot{e}_y/e_y)$ , and the output fuzzy variable  $k$  is the slope constant of the sliding surface. The membership functions are designed in a triangular form for the fuzzification of the input and output variables. The triangular membership functions of input and output fuzzy sets are shown in Fig. 4. The fuzzy inference rules are shown as follows:

**Rule 1:** IF  $-\dot{e}_y/e_y$  is N THEN  $k$  is  $k_1$

**Rule 2:** IF  $-\dot{e}_y/e_y$  is Z THEN  $k$  is  $k_2$

**Rule 3:** IF  $-\dot{e}_y/e_y$  is P1 THEN  $k$  is  $k_3$

**Rule 4:** IF  $-\dot{e}_y/e_y$  is P2 THEN  $k$  is  $k_4$

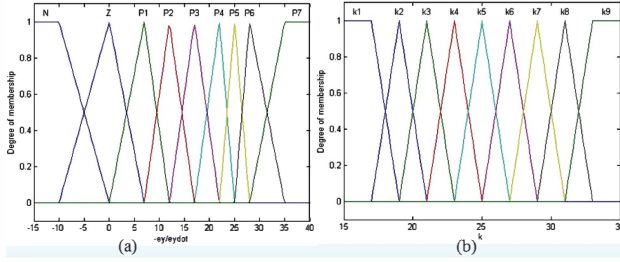


Fig. 4. Membership functions of the fuzzy sets for tuning sliding surface slope  $k$ .

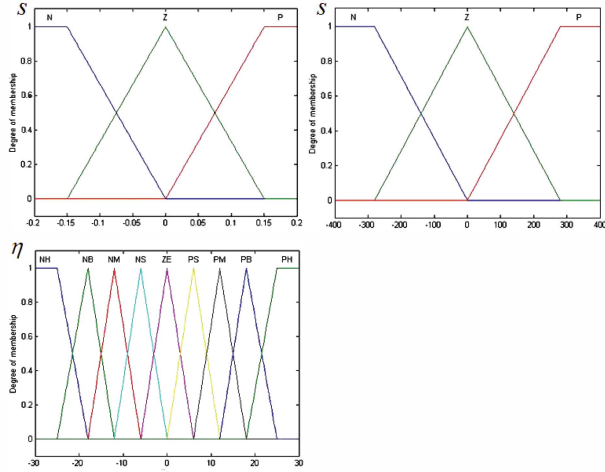


Fig. 5. Membership functions of the fuzzy sets for tuning switching control gain  $\eta$ .

- Rule 5:** IF  $-\dot{e}_y/e_y$  is P3 THEN  $k$  is k5  
**Rule 6:** IF  $-\dot{e}_y/e_y$  is P4 THEN  $k$  is k6  
**Rule 7:** IF  $-\dot{e}_y/e_y$  is P5 THEN  $k$  is k7  
**Rule 8:** IF  $-\dot{e}_y/e_y$  is P6 THEN  $k$  is k8  
**Rule 9:** IF  $-\dot{e}_y/e_y$  is P7 THEN  $k$  is k9

When it is in sliding mode, in order to have a stable motion on the sliding surface, the slope constant  $k$  must be positive definite. The slope constant of the sliding surface value  $k$  is kept in the stable region, so that the Lyapunov stability property of the control system is sustained.

In the second fuzzy inference mechanism of the controller, the input fuzzy variables are the sliding surface  $s$  and derivative of sliding surface  $\dot{s}$ , and the output fuzzy variable is the upper bound of the lumped uncertainty  $\eta$ . The membership functions are designed in a triangular form for the fuzzification of the input and output variables. The triangular membership functions of the fuzzy inputs and output are shown in Fig. 5. The fuzzy inference rules are shown as follows:

- Rule 1:** IF  $s$  is P and  $\dot{s}$  is P THEN  $\eta$  is NH  
**Rule 2:** IF  $s$  is P and  $\dot{s}$  is Z THEN  $\eta$  is NB  
**Rule 3:** IF  $s$  is P and  $\dot{s}$  is N THEN  $\eta$  is NM  
**Rule 4:** IF  $s$  is Z and  $\dot{s}$  is P THEN  $\eta$  is NS  
**Rule 5:** IF  $s$  is Z and  $\dot{s}$  is Z THEN  $\eta$  is ZE  
**Rule 6:** IF  $s$  is Z and  $\dot{s}$  is N THEN  $\eta$  is PS  
**Rule 7:** IF  $s$  is N and  $\dot{s}$  is P THEN  $\eta$  is PM

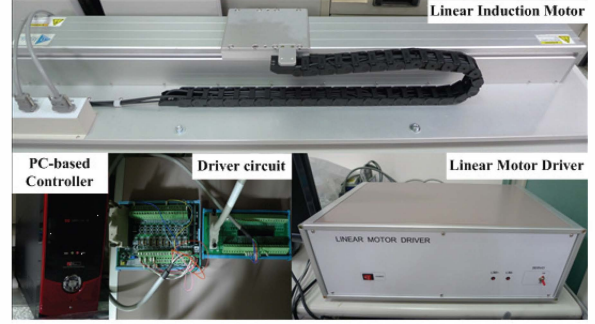


Fig. 6. Photo of the experimental platform.

TABLE I. LIM SPECIFICATIONS AND PARAMETERS

Rated specification		Parameters	
Pole pair	4	$M$	2.3 kg
Power	1 HP	$D$	40.95 kg/s
Voltage	240 V	$L_m$	0.085 H
Current	3A	$L_{r,s}$	0.1021 H
Secondary length	0.8 m	$R_r$	3.784 $\Omega$
		$R_s$	6.2689 $\Omega$

**Rule 8:** IF  $s$  is N and  $\dot{s}$  is Z THEN  $\eta$  is PB

**Rule 9:** IF  $s$  is N and  $\dot{s}$  is N THEN  $\eta$  is PH

With these two fuzzy inference mechanisms, the proposed EFSMC scheme is established.

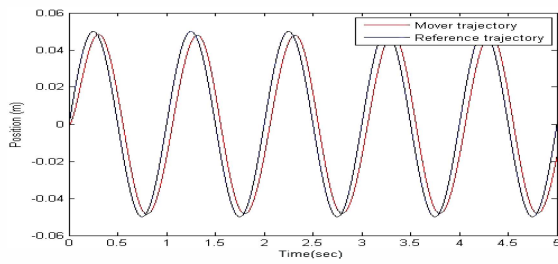
## V. EXPERIMENTAL RESULTS

As shown in Fig. 6, the experimental platform includes a LIM, a linear motor driver, a driver circuit, and a PC-based controller. The LIM is a three phase motor which is manufactured by Akribis Company, and its specifications and parameters are listed in Table I. Moreover, the resolution of the linear encoder is 1  $\mu\text{m}$ , and the maximum speed of mover is 5 m/s. The driver circuit is used to transmit the data between the PC and the driver. The PC uses Simulink software to implement the control law the interface between software and hardware.

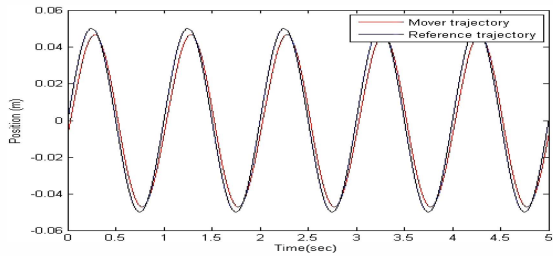
In this following, the experimental reference signal uses sine wave with amplitude of 5 cm, frequency of 1 Hz. Moreover, the experimental parameter gains of the PID controller and the conventional sliding mode controller are chosen as follows:  $k_p = 55$ ,  $k_i = 10$ ,  $k_d = 0.1$ ,  $k = 25$ ,  $\eta = 15$ ,  $\gamma = 30$ . Figure 7 shows the sine wave position tracking response of the following four control schemes: PID controller, SMC, and EFSMC. Figure 8 shows the control effort of the proposed control schemes, respectively. One can observe that the EFSMC schemes not only reduce the chattering phenomenon, but also decrease the value of control effort.

## VI. CONCLUSION

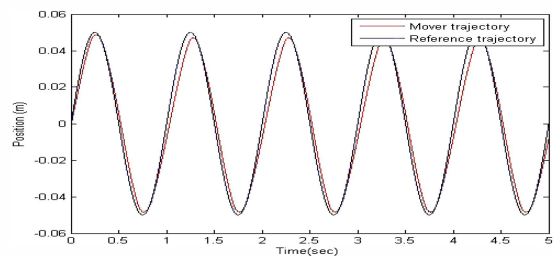
The design of an EFSMC with a flux observer is proposed in this paper. Considering the dynamic model of the LIM drive based on the indirect field-oriented control scheme with the end effect, a flux observer is designed to estimate the secondary flux for the LIM and further to use the inverse secondary time constant to calculate the compensation effort against the end effect. In addition, the proposed EFSMC is developed by integrating the Lyapunov stability theorem and fuzzy logic control to



(a) PID controller.

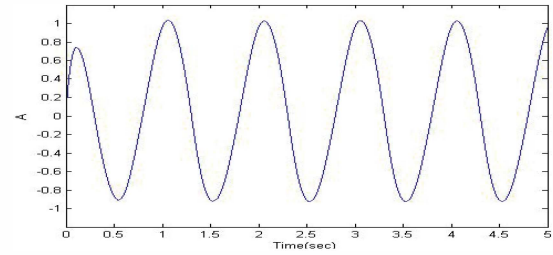


(b) SMC controller.

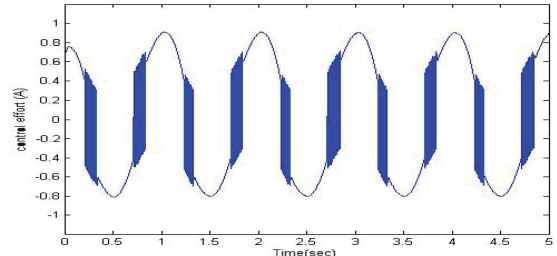


(c) EFSMC controller.

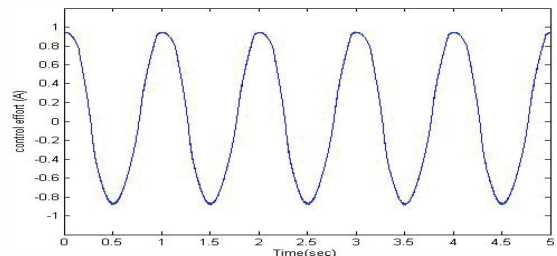
Fig. 8. Sinusoidal position tracking.



(a) PID controller.



(b) SMC controller.



(c) EFSMC controller.

Fig. 9. Control effort in sinusoidal position tracking.

adjust the controller parameters automatically, and also the ability to confront with the external disturbance and the unknown uncertainties. Through the experimental comparison with the conventional controllers of the PID and the SMC control, the EFSMC system exhibits the superior tracking performance and maintains the lower power consumption to a desired degree in the control effort.

#### REFERENCES

- [1] B. J. Lee, D. H. Koo, and Y. H. Cho, "Investigation of linear induction motor according to secondary conductor structure," *IEEE Transactions on Magnetics*, vol. 45, no. 6, pp. 2839-2842, June 2009.
- [2] F. J. Lin, C. K. Chang, and P. K. Huang, "FPGA-based adaptive backstepping sliding-mode control for linear induction motor drive," *IEEE Transactions on Power Electronics*, vol. 22, no. 4, pp. 1222-1231, July 2007.
- [3] F. J. Lin, L. T. Teng, C. Y. Chen, and Y. C. Hung, "FPGA-based adaptive backstepping control system using RBFN for linear induction motor drive," *Electric Power Applications, IET*, vol. 2, no. 6, pp. 325-340, Nov. 2008.
- [4] A. Zare Bazghaleh, M. Naghashan, H. Mahmoudimanesh and M. Meshkatoddini, "Effective design parameters on the end effect in single-sided linear induction motors," *World Academy of Science, Engineering and Technology (WASET)*, vol. 64, pp. 95-100, 2010.
- [5] W. J. Wang and J. Y. Chen, "A new sliding mode position controller with adaptive load torque estimator for an induction motor," *IEEE Transactions on Energy Conversion*, vol. 14, no. 3, pp. 413-418, Sep. 1999.
- [6] N. Sadati and A. Talasaz, "Chattering-free adaptive fuzzy sliding mode control," in *Proc. 2004 IEEE Conference on Cybernetics and Intelligent Systems*, vol. 1, pp. 29-34, Dec. 2004.
- [7] D. Antić, M. Milojković, S. Nikolić and S. Perić, "Optimal fuzzy sliding mode control with a time-varying sliding surface," in *Proc. 2010 International Joint Conference on Computational Cybernetics and Technical Informatics (ICCC-CONTI)*, pp. 149-153, May 2010.
- [8] F. J. Lin, D. H. Wang, and P. K. Huang, "FPGA-based fuzzy sliding-mode control for a linear induction motor drive," *IEEE Proceedings - Electric Power Applications*, vol. 152, no. 5, pp. 1137-1148, Sep. 2005.
- [9] I. K. Bousserhane, A. Boucheta, A. Hazzab, B. Mazari, M. Rahli and M. K. Fellah, "Fuzzy-sliding controller design for single sided linear induction motor position control," in *Proc. The International Conference on EUROCON, 2007*, pp. 1942-1947, Sep. 2007.
- [10] P. Hamedani and A. Shoulaie, "Indirect field oriented control of linear induction motors considering the end effects supplied from a cascaded H-bridge inverter with multiband hysteresis modulation," in *Proc. 4th Power Electronics, Drive Systems and Technologies Conference (PEDSTC)*, pp. 13-19, Feb. 2013.
- [11] Jianqiang Liu, Fei Lin, Zhongping Yang and T. Q. Zheng, "Field oriented control of linear induction motor considering attraction force & end-effects," in *Proc. CES/IEEE 5th International Power Electronics and Motion Control Conference*, vol. 1, pp. 1-5, Aug. 2006.
- [12] B. Bessaih, A. Boucheta, I. K. Bousserhane, A. Hazzab and P. Sicard, "Speed control of linear induction motor considering end-effects compensation using rotor time constant estimation," in *Proc. 9th International Multi-Conference on Systems, Signals and Devices (SSD)*, pp. 1-7, Mar. 2012.
- [13] H. T. Lee, L. C. Fu, and H. S. Huang, "Sensorless speed tracking control of induction motor with unknown torque based on maximum power transfer," *IEEE Transactions on Industrial Electronics*, vol. 49, no. 4, pp. 911-924, Aug. 2002.